5208 *Macromolecules* **2009**, *42*, 5208–5214
DOI: 10.1021/ma900566d

Macromolecules
ARTICLE

Mechanism of Cryopolymerization: Diffusion-Controlled Polymerization in a Nonfrozen Microphase. An NMR Study

Harald Kirsebom,[†] Gabriel Rata,[‡] Daniel Topgaard,[‡] Bo Mattiasson,[†] and Igor Yu. Galaev*,[†]

[†]*Department of Biotechnology, Lund University, SE-221 00 Lund, Sweden, and* [‡]*Department of Physical Chemistry 1, Lund University, SE-221 00 Lund, Sweden*

Received March 16, 2009; Revised Manuscript Received May 27, 2009

ABSTRACT: Polymerization of dimethylacrylamide (DMAAm) cross-linked with PEG diacrylate was studied using ^{1}H NMR both *in situ* in a semifrozen system and in a supercooled aqueous system. The amount of nonfrozen microphase, in which polymerization proceeds, is defined by the concentration of the starting monomers and the freezing temperature, which depends on the depression in freezing temperature caused by dissolved osmolytes. However, despite there being identical initial concentrations in the nonfrozen microphase, at a chosen temperature of −10 °C the cryopolymerization proceeded at different rates depending on the size of the nonfrozen microphase. Further studies of the conditions in the nonfrozen microphase were performed by using pulsed gradient spin echo (PGSE) to study the self-diffusion of solutes. Observations regarding the reaction rate were rationalized in terms of different degrees of long-range diffusion which was seen using PGSE. Cryopolymerization resulted in decreasing osmolyte concentration, and hence in gradual freezing of excess water as defined by the depression in freezing point caused by the remaining monomers. The NMR data provide a way of rationale predicting the effect of the monomer concentrations and freezing temperatures on the amount of nonfrozen microphase and its polymer concentration. These parameters define cryogel properties such as mechanical strength and porosity, which are evaluated using SEM and as flow resistance of cryogels.

Introduction

Use of the cryogelation technique to prepare macroporous materials for various applications, e.g., purification of proteins,[1,2] bioreactors,[3] tissue engineering,[4] enzyme immobilization,[5] and water purification,[6] is growing steadily. This technique is based on the formation of a polymeric structure in a semifrozen system in which solvent crystals act as a porogen. When a mixture containing the monomers and initiators is frozen, the solute molecules are expelled from the growing ice crystals[7] and are concentrated in a small, nonfrozen liquid phase. The same phenomenon of expulsion of solutes by a growing ice crystal occurs when freezing seawater with the salt gets expelled from the growing ice and accumulates in a liquid phase between the ice crystals.[8] The concentration of solutes during the freezing process in the nonfrozen part of the sample, frequently referred to as the *nonfrozen liquid phase*, is known as *cryoconcentration*.[9] The polymerization proceeds in this cryoconcentrated nonfrozen liquid phase that surrounds the ice crystals; thus, a dense polymeric gel is formed around these crystals. When the system is defrosted, the ice crystals melt and a macroporous interconnected network is formed which is complementary to the ice crystals. Pores in these cryogels are normally between 1 and 100 μm in diameter, depending on the freezing temperature, on the concentration of starting solution, and on the precursor material used.[10] The interconnectivity of the structure is a result of the growth of the ice crystals until they become connected with the facet of another ice crystal.[11]

As cryogels are finding more and more practical application, it is extremely important to have a better understanding of how different parameters affect the properties of the final cryogel. It is challenging to continuously monitor the cryopolymerization reaction as it proceeds in a heterogeneous system (ice crystals and nonfrozen liquid phase), which looks more like a solid piece of ice. The freezing process has been studied by controlling the sample temperature using a thermocouple;[12,13] however, the temperature measurement interferes with the freezing process itself since a probe is placed in the reaction medium. Alternatively, the polymerization reaction can be stopped at specific time points and the gel yield can be determined after defrosting.[14] Neither of these techniques allows continuous monitoring of the progress of polymerization.

Although NMR studies of polymerization reactions in liquid media are well-known,[15,16] there had only been sporadic attempts at using NMR for the study of cryogelation[17] until recently, when ^{1}H NMR was demonstrated as a suitable method for continuous study of the polymerization reaction in a semifrozen state.[18] The use of ^{1}H NMR permits simultaneous monitoring of the freezing process as well as the polymerization process without interfering with the sample. In the present study using ^{1}H NMR, we investigated the mechanism of cryopolymerization of dimethylacrylamide (DMAAm) cross-linked with PEG diacrylate by examining the effects of freezing (as compared to a supercooled nonfrozen system), monomer concentration, and freezing temperature on the rate of the polymerization reaction and the properties of the gels obtained. Further ^{1}H NMR diffusion experiments were carried out to provide additional information on the mechanism of cryopolymerization.

Experimental Section

Materials. *N*,*N*,*N*′,*N*′-Tetramethylethylenediamine (TEMED), ammonium persulfate (APS), DMAAm, PEG diacrylate (average molecular weight 258 g mol^{-1}), and silver iodide (AgI) were all obtained from Aldrich. Milli-Q-purified water was used for the preparation of all solutions.

*Corresponding author. E-mail: Igor.galaev@biotek.lu.se.

 Published on Web 07/02/2009

Preparation of Gels. Gels were prepared by dissolving DMAAm and PEG diacrylate (mol ratio 60:1) to final concentrations of 3, 6, or 12% (w/v) in Milli-Q-purified water and the solutions were degassed under vacuum to remove dissolved oxygen. Then TEMED (2% of total monomer weight) was added and the samples were kept in an ice bath. Finally, APS (2% of total monomer weight) was added and 400 μL of the solution was transferred to an NMR tube (diameter 5 mm). The sample was then polymerized either at +4, −10, or −20 °C. In order to freeze the samples, a few crystals of AgI were added to the NMR tube before adding monomer solution. The samples polymerized under supercooled conditions at −10 °C were prepared in the same way except that no AgI was added to the tubes. The samples were either polymerized *in situ* in the NMR tubes at the set temperature or in an ethanol-cooled cryostat (Lauda RK20KP).

NMR Measurements. The measurements were carried out with a Bruker AVII 200 MHz spectrometer. The spectrometer was equipped with a Bruker DIF-25 probe, with a maximum gradient strength of 9.63 T/m, and fitted with a 5-mm radio-frequency (RF) coil. ^{1}H spectra were recorded with a 90° pulse sequence, with a recycle delay of 1 s, 4 scans, and a 90° pulse length of 12 μs. The time required for recording one spectrum was 5 s, and the spectra were acquired every 25 s for the first 30 min, and thereafter spectra were acquired with 10-min delay for a total time of about 14 h. The reaction mixture, prepared as described above, was immediately monitored under controlled temperature at −10 and −20 °C, under frozen and supercooled conditions.

The chemical shift of the spectra was calibrated by setting the signal of the methyl group in DMAAm to 3.1 ppm.[19] A number of Lorentzian functions were fitted to the spectrum in order to quantify the area of the peaks under study, fits were done in matlab (Matlab, The MathWorks, Natick, MA.). The peak corresponding to a vinyl proton at 6.9 ppm for the monomer (DMAAm) and the water peak, at 4.7 ppm was used to monitor the change in the concentrations (Figure 1). The resonance line at 6.9 ppm was selected for DMAAm since the separation from the water peak is greatest. The cross-linker PEG diacrylate is not clearly visible in the spectrum due to the low concentration used.

To study the conditions for the polymerization reaction further, diffusion measurements were used. The pulse sequence used in this case was pulsed gradient stimulated echo (PGSTE, $\pi/2-\tau_1-\pi/2-\tau_2-\pi/2-\tau_1-$echo). The diffusion coefficient is calculated with the classical Stejskal−Tanner equation[20]

$$I/I(0) = \exp(-\gamma^2\delta^2G^2Dt_{\mathrm{diff}}) \quad (1)$$

where I and $I(0)$ are the intensities with applied gradient and in the absence of applied gradient, γ is the gyromagnetic ratio, D is the diffusion coefficient, G is the gradient strength, and δ is the duration of the gradient pulse. The effective diffusion t_{diff} can be expressed in the following equation:[21]

$$t_{\mathrm{diff}} = \Delta - \frac{\delta}{3} - \frac{\varepsilon^3}{30\delta^2} - \frac{\varepsilon^2}{6\delta} \quad (2)$$

Here Δ is the interval between the leading edges of the two gradient pulses and ε is the ramp time; the gradient pulses are of trapezoidal shape. In the case of the diffusion measurements they have been carried out at −10 °C under frozen conditions for 3%, 6%, and 12% initial reactant solution without the addition of APS and under supercooled conditions for 6% and 33% reactant solution. The parameters for the PGSTE were 32 scans, recycle delay of 3 s, 90° pulse length 12 μs, δ of 1 ms, and ε 0.01 ms. Diffusion time varied from 50 ms to 1 s, which resulted in a experimental time of 30 min for each Δ (using a variable field-gradient strength of maximum 9.63 T/m). For these measurements the maximum gradient strengths used were decreased from 2.9 T/m to 0.24 T/m when increasing the value of Δ. For each Δ, the gradient was increased in logarithmic steps from 2% to 100% of the value of the maximum used gradient in 16 increments.

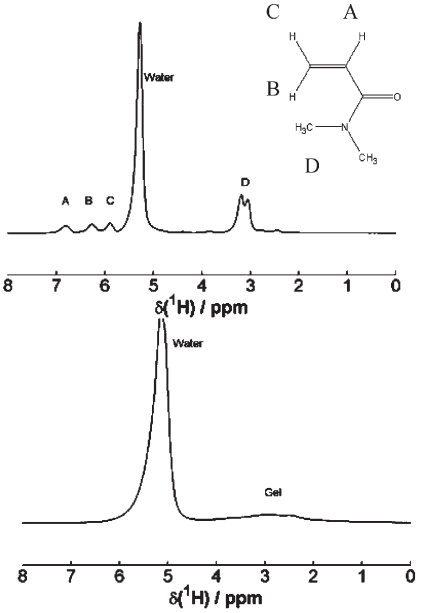

Figure 1. Acquired spectra for DMAAm-*co*-PEG diacrylate at −10 °C. Spectrum for semifrozen system before reaction (top) and spectrum after polymerization was complete (bottom). The signals for DMAAm are assigned to the peaks in the prepolymerization spectrum.

The maximum used gradient values were different for the different concentrations, with larger gradient values for higher concentrations. The diffusion coefficient was evaluated by fitting the signal using a monoexponential decay in matlab (Matlab, The MathWorks, Natick, MA). The samples had been equilibrated at the temperature studied for 1 h prior to the first diffusion experiment.

Characterization of Cryogels. Prepared samples were cut into thin discs for scanning electron microscopy (SEM) and they were fixed in 2.5% glutaraldehyde solution in 0.1 M sodium phosphate buffer (pH 7.4) overnight at 4 °C. They were dehydrated in ethanol (0%, 20%, 75%, 95%, and 99.5%) and then critical-point dried. The dried samples were sputter-coated with gold/palladium (40/60) and examined using a JEOL JSM-5000LV scanning electron microscope. The average pore sizes of the samples were calculated by measuring at least 50 pores of each sample using Image J software (NIH image).

Cryogels prepared in an NMR tube were cut into pieces 5 mm in length and used for compression analysis. Compression tests were performed using a TA-XT2 instrument (Stable Micro Systems, Godalming, Surrey, U.K.) at ambient temperature, using a 25-mm diameter plunger. Samples were compressed to 70% deformation and the elasticity modulus was calculated at a deformation of 40% using the following equation:

$$E = (F/A)/(\Delta l/l) \quad (3)$$

Here E is the elasticity modulus (Pa), F is the applied force (N), A is the area of sample (m^2), Δl is the change in length (m) at compression, and l is the initial length (m). Five measurements were made for each sample, and the average is shown.

The flow rate of water passing through the gel was measured at a constant water pressure equal to a 50-cm column of water. Measurements were done in triplicate for each sample.

Results and Discussion

Cryopolymerization is polymerization in a semifrozen state, which results in polymeric systems of significantly different

Table 1. (Cryo)Polymerization of 6 wt % DMAAm-*co*-PEG Diacrylate at Different Temperatures

sample	amount of nonfrozen water (wt %)	concentration in liquid phase (wt %)	expected concentration[a] (M)	time until reaction start (min)	time of reaction (min)
+4 °C	100	6.0 (0.59 M)	0.59	70	55
−10 °C (supercooled)	100	6.0 (0.59 M)	0.59	370	80
−10 °C	11.6	32.6 (3.2 M)	3.46	260	100
−20 °C	7.0	45.5 (4.47 M)	5.09	950	800

[a] The concentration is calculated using eq 4 and shows the expected concentration, which would correspond to the depression in the freezing point.

morphology than those from polymerization in homogeneous solution. The mechanism behind this is not completely understood. It is believed[9] that polymerization in a semifrozen state proceeds in liquid microphase, composed of the cryoconcentrated solution of the solutes present in the system. Thus, the polymerization proceeds under very unusual conditions of temperature below zero, high concentration of monomers, and space constraints with high surface-to-volume ratio. A recently developed technique[18] for monitoring cryopolymerization *in situ* using ^{1}H NMR allows study of the influence of the initial monomer concentration and freezing temperature on the polymerization rate, in order to better understand—and hence control in a more rational way—the properties of the cryogels produced.

As a model system, the copolymerization of DMMAm-PEG diacrylate (60:1 mol ratio) was selected since DMAAm contains no labile protons, and this minimizes the exchange with water (Figure 1). A low ratio of PEG diacrylate was selected to minimize the signal obtained from this cross-linker while still producing cross-linked gels. Comparison of the polymerization in semifrozen and supercooled conditions enables studies of the influence of the presence of an ice matrix during the reaction, both in terms of the reaction progress and the properties of the (cryo)gels obtained.

The Influence of Freezing. (Cryo)polymerization of DMMAm-PEG diacrylate (60:1 mol ratio) from a 6 wt % feed was studied at −10 °C. At this temperature, the system can either be in a supercooled and hence metastable liquid state[22] or in a semifrozen condition when freezing is induced by adding a few crystals of AgI into the NMR tube before the addition of the monomeric solution. Crystals of AgI provide nucleation sites at which the ice crystals can start to grow, and they thus promote freezing. AgI is not soluble in the polymerization medium and so it does not affect the reaction; nor does the AgI influence the NMR measurements.

The volume of the nonfrozen phase is determined by the initial concentration of solutes (osmolytes) and the temperature used. For example, the volume of nonfrozen microphase in a 0.4 mL sample is approximately 44 μL for the system with a 6 wt % monomer concentration at −10 °C. Solutes are concentrated in the nonfrozen phase until the depression in freezing point due to the increased concentration is equal to the temperature used. Freezing-point depression of an ideal solution can be calculated with the following equation, and can be used as an estimation to describe the system used:[23]

$$\Delta T = K_f b \tag{4}$$

where ΔT is the depression in freezing point, K_f is the cryoscopic constant for water (1.86 K kg mol^{-1}), and b is the molality of the solutes. Table 1 shows the actual concentrations in the nonfrozen liquid phase obtained from ^{1}H NMR signals of nonfrozen water and from monomers, and also the theoretically expected concentrations calculated using eq 4. Concentrations were calculated as the ratio between the area of the vinyl peak at 6.9 ppm and the area of the water peak. It is assumed that only the water freezes and the monomer remains liquid. The experimental and theoretical concentrations show good agreement at −10 °C, although some deviation can be expected due to nonideality of the monomer solution with deviations becoming more pronounced at higher monomer concentrations.[24]

The polymerization reaction in the supercooled system can be considered to be a classical radical cross-linking polymerization reaction in a liquid phase. However, the reaction in the semifrozen state will most likely proceed under different condition.

It could be expected that as polymerization proceeds, the water freezes rapidly and keeps the concentration of solutes in the nonfrozen phase constant in order to maintain the freezing-point depression constant corresponding to the surrounding temperature. However, this is not what is observed in Figure 2 which shows the change of monomer/water signal ratio in the systems at −10 °C both for the semifrozen and supercooled systems, respectively. The ratio of monomer/water signals can be considered as an estimation of the monomer concentration in nonfrozen microphase. Clearly the concentration changes over time and is not constant, this is most likely due to the fact as the monomer concentration decrease and more water should thus freeze (eq 4). However as monomers are consumed the gel is formed and will give rise to nonfrozen water due to the hydration of the gel.[25]

The cryoconcentration effect where the monomers are concentrated in the liquid phase due to the formation of ice crystals was studied at −10 °C. For the 6 wt % sample, it was possible to carry out the polymerization reaction both in (supercooled) liquid and in a semifrozen system. This allows study of the reaction at the same temperature. However, under supercooled conditions the monomer concentration in the liquid phase is 6 wt % whereas in the semifrozen system the concentration is approximately 33 wt % in the nonfrozen phase (Table 1). Thus, the polymerization for these two systems proceeds under substantially different conditions even though the initial condition (before freezing) and the reaction temperature are the same (Figure 2). Not surprisingly, the resulting (cryo)gels were very different. A heterogeneous, spongy, elastic, opaque cryogel was produced in the semifrozen system whereas a homogeneous brittle gel was produced under supercooled conditions (Figure 3). The structure and physical properties of the gel produced under supercooled conditions were close to that of a gel produced at ambient temperature, whereas the properties of a cryogel are defined by macropores (produced in place of melted ice crystals) and pore walls composed of concentrated polymer phase (produced as the result of polymerization in cryoconcentrated solution).

The rate of initiation of the reaction depends on the initiator concentration[26]

$$R_i = 2fk_d[I] \tag{5}$$

where R_i is the rate of initiation, f is the efficiency of the initiation, k_d is the rate constant of decomposition of the initiator, and [I] is the concentration of the initiator. Thus, the cryoconcentration of the initiator along with the cryoconcentration of monomers promotes earlier onset of the

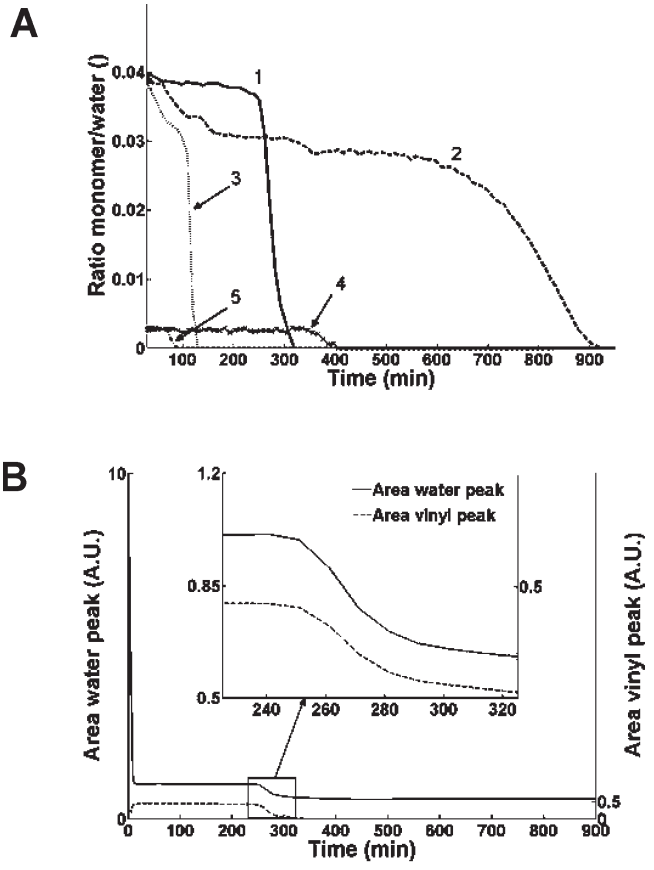

Figure 2. (A) Change in monomer concentrations for (cryo)polymerization of DMAAm-*co*-PEG diacrylate (approximated as the ratio of monomer and water NMR signals) in different (cryo)polymerization systems as a function of time: (1) 3% (−10 °C), (2) 6% (−10 °C), (3) 12% (−10 °C), (4) 6% (+4 °C), and (5) 6% (−10 °C supercooled). (B) Changes in water peak area and vinyl peak area as a function of time. Reaction rate was calculated from A as the change in ratio of monomer/water over time during the period of main monomer consumption (at maximum derivative). The onset of polymerization is set as the time when the main consumption of monomers start (a decrease of more than 0.01 units of monomer signal per 10 min) and the reaction time is the time from the main consumption of monomers starts until the concentration reaches zero.

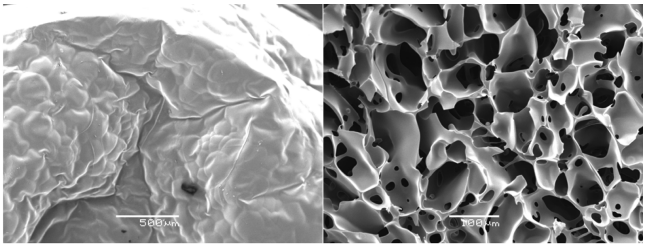

Figure 3. SEM images of a DMAAm-*co*-PEG (60:1) gel (left) prepared from a 6 wt % feed at −10 °C in a supercooled system, and cryogel prepared from a 6 wt % feed in a semifrozen system (right).

polymerization in the semifrozen system after 260 min as compared to the supercooled system, in which polymerization starts only after 370 min.

The reaction times for supercooled and semifrozen systems are similar despite significant differences in the concentration: 6 and 33 wt %, respectively. The 5.5-fold higher monomer concentration in the semifrozen system would make the polymerization considerably faster than that in the supercooled system due to concentration differences. However this is not the case (Figure 2A), and the reaction

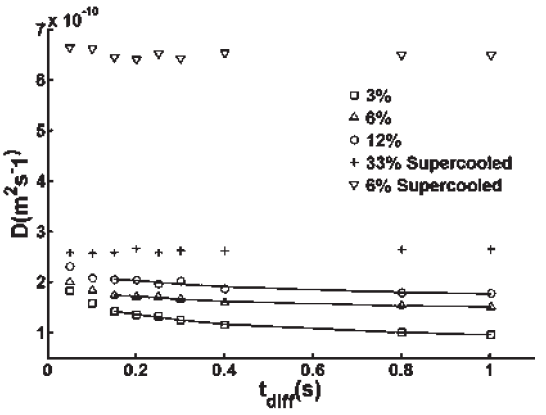

Figure 4. Apparent diffusion coefficient of water as a function of t_{diff} for semifrozen samples at −10 °C and supercooled samples, with different initial monomer concentrations. Lines indicate the fit of eq 7 for t_{diff} higher than 151 ms for the three semifrozen systems.

times are similar. One possible explanation for this could be related to diffusion in the system. Diffusion of molecules in confined spaces can either be considered for long or short time scales, at short time scales the short-range diffusion is equal to the bulk diffusion (D_0). Diffusion at longer time scales reaches a plateau value (D_∞) which depends on the connectivity of the pore space.[27] Differences in the diffusion in the supercooled and semifrozen system are both for the long-range diffusion (at high t_{diff}) and the short-range diffusion (at short t_{diff}). The diffusion at both long and short t_{diff} are significantly faster (Figure 4) for the supercooled system than for the semifrozen, which could explain the reaction times (see further discussions about the influence of diffusion below). At the studied t_{diff} (50 ms to 1 s) the studied molecules move in the range between 5 and 19 μm depending on the t_{diff} and the sample studied. This corresponds to the observed distances in the nonfrozen microphase which is visualized as the pore walls in the SEM images (Figure 3) and the sizes of the pores.

The Influence of Initial Monomer Concentration. Comparing the samples with initial concentrations of 3, 6, and 12 wt %, it is evident that the reactions start after different times and proceed at different rates (Figure 2), although the monomer/initiator concentrations were the same in all systems as defined by the depression in freezing point (eq 4, Table 2). Despite the fact that there were different initial concentrations before freezing, in all three systems the water froze with a concomitant increase in monomer concentration, until a sufficient concentration was reached that corresponded to the depression in freezing point.

Diffusion in semifrozen samples (with 33 wt % monomer concentration) was found to be slower than that in a similar (33 wt % monomer concentration) supercooled sample at −10 °C. Even if the systems studied were at same temperature and equal apparent concentration the observed diffusion was different. However, the diffusion coefficients observed for the semi frozen systems are different and dependent on diffusion time, t_{diff}, indicating that the diffusion is restricted on a longer time scale (Figure 4), while the supercooled system was independent of diffusion time. The diffusion in these semifrozen systems can be considered as diffusion in a porous medium and thus Archie's law[28] would be applicable. Archie's law describes the relation between the porosity of a sample and the long-range diffusion:

$$D_\infty = \varphi_t^{m_1} D_0 \qquad (6)$$

Table 2. (Cryo)Polymerization of DMAAm-*co*-PEG Diacrylate under Different Conditions

sample (feed concentration, temperature)	amount of nonfrozen water (%)	concentration in liquid phase (%)	time until reaction (min)	time of reaction (min)	D at Δ = 1000 ms ($m^2\ s^{-1}\ 10^{-10}$)
12 wt %, −10 °C	25.2	32.0 (3.14 M)	110	30	1.78
6 wt %, −10 °C	11.6	32.6 (3.20 M)	260	100	1.51
3 wt %, −10 °C	4.9	34.2 (3.36 M)	~600	300	0.96
6 wt %, −10 °C (supercooled)	100	6.0 (0.59 M)	370	80	6.43
6 wt %, −20 °C	7.0	45.5 (4.47 M)	950	800	0.22

where m_l is an empirical exponent specific for the liquid phase and depends both on the sample geometry and the wetting properties of the liquid, D_0 is the diffusion coefficient in bulk liquid, and φ_t is the porosity of the sample. Since the wetting properties of the liquid do not change and the filling factor is the same (the interstitial volume between ice crystals is filled completely with the liquid), the equation shows the dependence between the diffusion coefficient and the sample geometry, specifically the total porosity and pore size. The volumes of the nonfrozen phases for the different semifrozen samples are different (Table 2), and therefore, the larger pore size (the nonfrozen liquid phase is considered as pores in the ice matrix) observed in systems with higher initial monomer concentration results in a higher diffusion.

In a porous medium, the diffusion will reach D_0 at very short t_{diff}, however these small t_{diff} could not experimentally be probed. That results in the deviation between the three semifrozen systems and the 33% supercooled at short t_{diff}. The compositions of the three semifrozen systems are the same since the composition is only dependent on the temperature thus the D_0 should be the same for all samples. At long t_{diff} the diffusion can be described by the following equation:[29]

$$D(t_{diff}) = D_\infty + D_0\left(\frac{\beta_1}{t_{diff}} - \frac{\beta_2}{t_{diff}^{3/2}}\right) \quad (7)$$

Here $D(t_{diff})$ is the diffusion at time t_{diff} and β_1 and β_2 are constants depending on the geometry.

Fitting eq 7 to the data in Figure 4 gives an approximation of the D_∞ which can be correlated with the tortuosity of the systems (Table 3); the value for the D_0 used for the fitting was D for the 33% supercooled sample. The supercooled systems show no dependence on D at different t_{diff} which is characteristic for bulk diffusion while the three semifrozen systems show a D_∞ which is different from D_0 depending on the tortuosity of the semifrozen systems. The diffusion for the three semifrozen systems levels off at high t_{diff} and approaching D_∞ which is visible for the 12% sample while the 3% sample has not leveled off at the t_{diff} investigated (Table 3). The pores in the 3% sample are in the range of 50 μm. To be able to measure the estimated D_∞, values of t_{diff} over 10 s would be required. Such high values are not experimentally feasible due to the influence of T_1 relaxation. In the semifrozen system, the reaction rate correlates almost linearly with the long-range diffusion coefficient (Figure 5). Thus the long-range diffusion might partly explain the differences in reaction time as discussed above in relation to freezing of the system.

Diffusion measurements for the semifrozen system may be influenced by cross-relaxation between the liquid phase and the ice matrix. Cross-relaxation between a solid matrix and a liquid phase has previously be shown to influence the diffusion.[17,30,31] In order to verify whether any contribution to the diffusion measurements from the interactions between the ice and the liquid water exists, a Goldman−Shen experiment[32] was performed; this showed no transfer of magnetization between ice and nonfrozen water. Thus, the diffusion coefficients obtained can be used without corrections. As it might have been expected to observe some cross-relaxation between the ice and the liquid water phase, the lack of this effect may have been due to a smaller surface to volume ratio of the nonfrozen water in the studied systems than in systems were cross-relaxation has been observed.[17,30] A large interface area usually gives rise to high cross-relaxation;[31] however, cryogels have been shown previously to have a rather limited pore surface area.[33] The surface area of the cryogels is a good approximation of the ice−liquid interface area in semifrozen systems.

Table 3. Calculated Diffusion Data of the Systems Studied at −10 °C

sample (feed concentration)	$D_\infty(/D_0)^a$	D_∞ ($m^2\ s^{-1}\ 10^{-10}$)^a
12 wt %	0.63	1.63
6 wt %	0.54	1.40
3 wt %	0.29	0.76
6 wt % (supercooled)	1	6.43[b]
33 wt % (supercooled)	1	2.61[b]

[a] Values obtained from the fitting of eq 7 to data in Figure 4. [b] Values measured at 1000 ms.

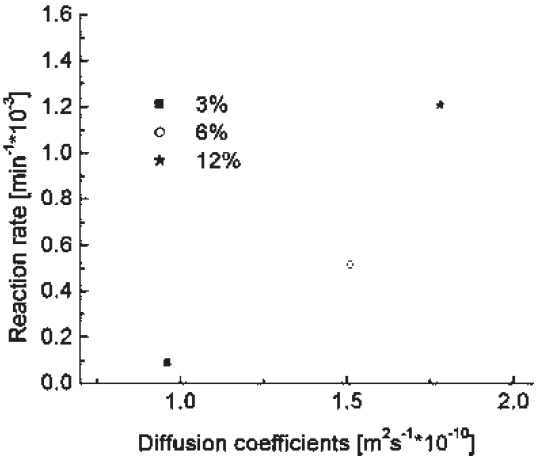

Figure 5. Relationship between diffusion coefficient (D_∞) and reaction rate for DMAAm-*co*-PEG diacrylate cryopolymerization in feeds with 3, 6, and 12 wt % monomer concentrations. Reaction rate was calculated from Figure 2A as the change in ratio of monomer/water over time during the period of main monomer consumption.

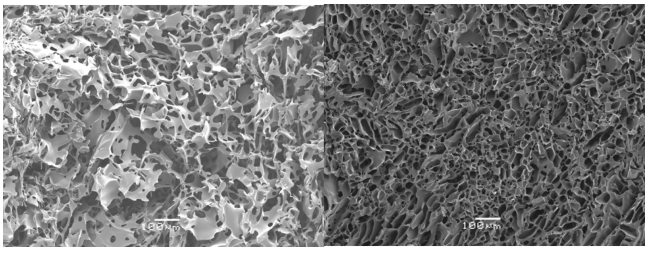

Figure 6. SEM images of DMAAm-*co*-PEG diacrylate cryogels prepared at −10 °C from a feed with monomer concentrations of 3 wt % (left) and with 12 wt % (right).

Table 4. Properties of the DMAAm-*co*-PEG Diacrylate Cryogels Prepared under Different Conditions

sample	average pore size (μm)	water flow rate (cm/h)	elasticity module (kPa)	yield (%)
12% (−10 °C)	18.0	90 ± 7	33.3	86
6% (−10 °C)	44.2	520 ± 47	5.3	90
3% (−10 °C)	52.1	605 ± 150[a]	[b]	80
6% (−20 °C)	25.0	210 ± 67	[b]	90

[a] Sample gets compressed because of the pressure and the observed value is lower due to the compression. [b] Samples were mechanically too weak to be used for compression measurements.

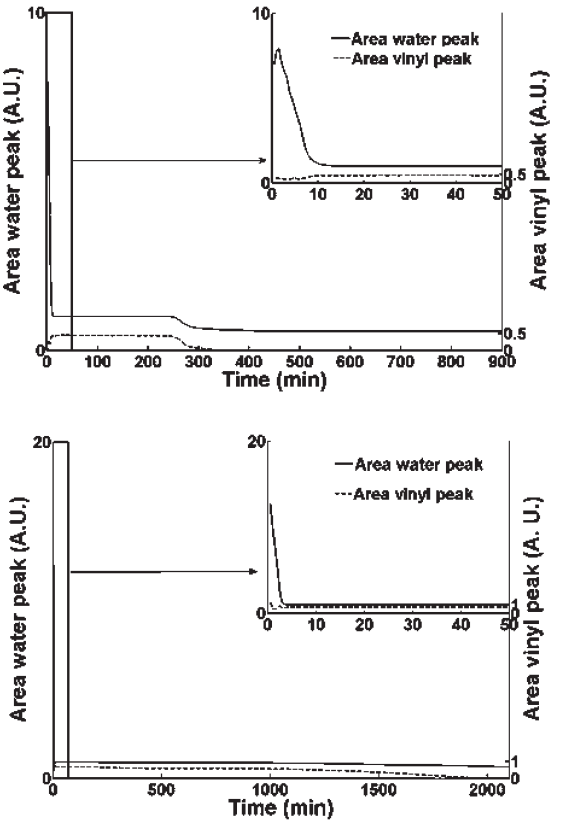

Figure 7. Evolution of water and monomer peaks as a function of time for DMAAm-*co*-PEG diacrylate cryopolymerization in the feed with 6 wt % monomer concentration; −10 °C (top) and −20 °C (bottom).

The difference in diffusion coefficients for three semifrozen systems clearly indicates the existence of different diffusion restrictions in liquid microphase, which are translated later on into different pore structures of the cryogels as the volume and shape of the liquid microphase define the structure of pore walls and total porosity in the cryogel after the ice crystals melt. Indeed, SEM images show much larger pores and thinner pore walls in the cryogel sample produced from 3 wt % feed as compared to cryogel produced form 12 wt % feed (Figure 6 and Table 4). Smaller pore size and thicker pore walls in cryogels prepared from 12 wt % feed resulted in significantly less flow of liquid through the cryogel, and a significant increase in the mechanical stability (elastic modulus) compared to the cryogels prepared from feeds with lower monomer concentration.

The Influence of Temperature. In the case of cryogels, the reaction temperature affects both the reaction rate and the structure obtained by influencing the amount of nonfrozen microphase and also the size of ice crystals formed when freezing. Lower freezing temperature results in faster freezing and a smaller nonfrozen liquid phase (Figure 7). More ice nucleation sites result in more ice crystals, but they are smaller in size.

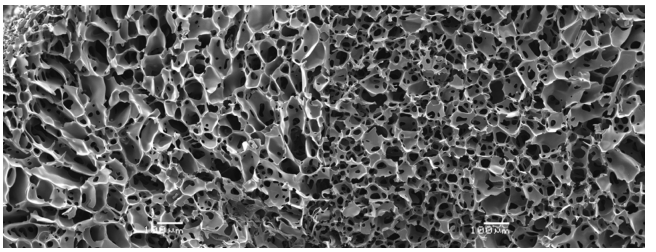

Figure 8. SEM images of DMAAm-*co*-PEG prepared from the feed with 6 wt % monomer concentration at −10 °C (left) and at −20 °C (right).

Thus, a cryogel prepared at −20 °C appeared to have more pores of smaller size than a sample prepared at −10 °C, as indicated both by scanning SEM (Figure 8), and a lower flow rate of liquid compared to that for the cryogel prepared at −10 °C (Table 4). The polymerization reaction at −20 °C is slower than that at −10 °C, despite the fact that the concentration of monomers in nonfrozen microphase is higher at −20 °C than at −10 °C (45.5 wt % versus 32.6 wt %, respectively). The increased monomer concentration is probably not sufficient in this case to compensate for the decrease in reaction rate due to the drop in temperature (e.g., compare polymerization rates at 4 °C and under supercooled conditions at −10 °C, Figure 2A) and the reduction in reaction rate due to increased limitation of diffusion under these conditions (Table 2). It could be expected that the concentration of polymer in the pore walls would be higher for the cryogel prepared at −20 °C than for the sample prepared at −10 °C due to the higher concentration of monomers in the nonfrozen liquid phase. However, the cryogels prepared at −20 °C are mechanically weaker than cryogels prepared at −10 °C.

In all the systems studied, there was no visible peak for the vinyl group after the polymerization reaction was completed; only a water peak and a broad gel peak were observed in the NMR spectra, indicating complete consumption of the monomers (Figure 1). However, the yields of the cryogels produced were 80−90%, indicating that some oligomers or polymer fragments were formed that were not bound covalently to the gel network and were subsequently washed out.

Conclusion

^{1}H NMR allows detailed monitoring of the polymerization process under semifrozen conditions, regarding both the change in the amount of liquid in the nonfrozen microphase and the concentration of monomers in it. The amount of nonfrozen microphase is defined purely by the initial monomer concentrations and the depression of freezing point. Cryopolymerization resulted in reduction of osmolyte concentration and hence a gradual decrease in the amount of nonfrozen microphase. However, cryopolymerization proceeds faster than excess water is frozen (as defined by freezing-point depression caused by remaining monomers). At high monomer concentrations in the nonfrozen microphase, the polymerization rate is highly dependent on molecular diffusion, which is in turn also affected by the amount of nonfrozen microphase in the sample. The NMR data

provide a way of predicting the effect of the monomer concentrations and freezing temperatures on cryogel properties such as mechanical strength and porosity as evaluated using SEM and flow resistance of cryogels.

Acknowledgment. This work was financially supported by Swedish Research Council (VR) and Swedish Foundation for Strategic Research (SSF). Part of the work was supported by the FP-6 Project Biomaterials for Wound Healing and Tissue Regeneration and the FP-7 Project Monolithic Adsorbent Columns for Extracorporeal Medical Devices and Bioseparations.

References and Notes

(1) Arvidsson, P.; Plieva, F. M.; Lozinsky, V. I.; Galaev, I. Yu.; Mattiasson, B. *J. Chromatogr. A* **2003**, *986*, 275–290.
(2) Yao, K. J.; Yun, J. X.; Shen, S. C.; Wang, L. H.; He, X. J.; Yu, X. M. *J. Chromatogr. A* **2006**, *1109*, 103–110.
(3) Kumar, A.; Bansal, V.; Nandakumar, K. S.; Galaev, I. Yu.; Roychoudhury, P. K. R.; Holmdahl, R.; Mattiasson, B. *Biotechnol. Bioeng.* **2006**, *93*, 636–646.
(4) Boelgen, N.; Plieva, F.; Galaev, I. Yu.; Mattiasson, B.; Piskin, E. *J. Biomater. Sci., Polym. Ed.* **2007**, *18*, 1165–1179.
(5) Lysogorskaya, E. N.; Roslyakova, T. V.; Belyaeva, A. V.; Bacheva, A. V.; Lozinskii, V. I.; Filippova, I. Y. *Appl. Biochem. Microbiol.* **2008**, *44*, 241–246.
(6) Le Noir, M.; Plieva, F.; Hey, T.; Guieysse, B.; Mattiasson, B. *J. Chromatogr. A* **2007**, *1154*, 158–164.
(7) Butler, M. F. *Cryst. Growth Des.* **2002**, *2*, 541–548.
(8) Worster, M. G.; Wettlaufer, J. S. *J. Phys. Chem. B* **1997**, *101*, 6132–6136.
(9) Lozinsky, V. I. *Russ. Chem. Rev.* **2002**, *71*, 489–511.
(10) Plieva, F. M.; Galaev, I. Yu.; Mattiasson, B. *J. Sep. Sci.* **2007**, *30*, 1657–1671.
(11) Savina, I. N.; Cnudde, V.; D'Hollander, S.; Van Hoorebeke, L.; Mattiasson, B.; Galaev, I. Yu.; Du Prez, F. *Soft Matter* **2007**, *3*, 1176–1184.
(12) Ivanov, R. V.; Lozinsky, V. I. *Polym. Sci. Ser. A* **2006**, *48*, 1232–1239.
(13) Plieva, F.; Xiao, H. T.; Galaev, I. Yu.; Bergenstahl, B.; Mattiasson, B. *J. Mater. Chem.* **2006**, *16*, 4065–4073.
(14) Lozinsky, V. I.; Vainerman, E. S.; Ivanova, S. A.; Titova, E. F.; Shtil'man, M. I.; Belavtseva, E. M.; Rogozhin, S. V. *Acta Polym.* **1986**, *37*, 142–146.
(15) Ito, H.; Dalby, C.; Pomerantz, A.; Sherwood, M.; Sato, R.; Sooriyakumaran, R.; Guy, K.; Breyta, G. *Macromolecules* **2000**, *33*, 5080–5089.
(16) Aguilar, M. R.; Gallardo, A.; Fernandez, M. D.; San Roman, J. *Macromolecules* **2002**, *35*, 2036–2041.
(17) Topgaard, D.; Soderman, O. *Biophys. J.* **2002**, *83*, 3596–3606.
(18) Kirsebom, H.; Rata, G.; Topgaard, D.; Mattiasson, B.; Galaev, I. Yu. *Polymer* **2008**, *49*, 3855–3858.
(19) Nakahama, S.; Kobayashi, M.; Ishizone, T.; Hirao, A.; Kobayashi, M. *J. Macromol. Sci. A* **1997**, *34*, 1845–1855.
(20) Stjejskal, E. O; Tanner, J. E. *J. Chem. Phys.* **1965**, *42*, 288–292.
(21) Price, W. S. *Concepts Magn. Reson.* **1998**, *10*, 197–237.
(22) Ludwig, R. *Angew. Chem., Int. Ed.* **2006**, *45*, 3402–3405.
(23) Atkins, P. W., *Physical Chemistry*, 6th ed.; Oxford University Press: Oxford, U.K., 2001.
(24) Fullerton, G. D.; Keener, C. R.; Cameron, I. L. *J. Biochem. Biophys. Methods* **1994**, *29*, 217–235.
(25) Wolfe, J.; Bryant, G.; Koster, K. L. *CryoLetters* **2002**, *23*, 157–166.
(26) Sun, S. F., *Physical Chemistry of Macromolecules Basic Principles and Issues*, 2nd ed.; Wiley Interscience: NJ, 2004.
(27) Valiullin, R.; Skirda, V. *J. Chem. Phys.* **2001**, *114*, 452–458.
(28) Ardelean, I.; Farrher, G.; Mattea, C.; Kimmich, R. *Magn. Reson. Imaging* **2005**, *23*, 285–289.
(29) Latour, L. L.; Kleinberg, R. L.; Mitra, P. P.; Sotak, C. H. *J. Magn. Reson.* **1995**, *112*, 83–91.
(30) Topgaard, D.; Soderman, O. *Langmuir* **2001**, *17*, 2694–2702.
(31) Valiullin, R.; Furo, I. *J. Chem. Phys.* **2002**, *117*, 2307–2316.
(32) Goldman, M.; Shen, L. *Phys. Rev.* **1996**, *144*, 321–331.
(33) Plieva, F. M.; Karlsson, M.; Aguilar, M. R.; Gomez, D.; Mikhalovsky, S.; Galaev, I. Yu. *Soft Matter* **2005**, *1*, 303–309.